NJC

PAPER

View Article Online
View Journal | View Issue

Cite this: *New J. Chem.*, 2016, **40**, 10153

Effects of the incorporation of bithiophene instead of thiophene between the pyrrolo[3,4-*c*]pyrrole-1,3-dione units of a bis(pyrrolo[3,4-*c*]pyrrole-1,3-dione)-based polymer for polymer solar cells

Vellaiappillai Tamilavan,[ab] Seungmin Kim,[b] Ji Yeong Sung,[a] Dal Yong Lee,[b] Shinuk Cho,[c] Youngeup Jin,[d] Junghyun Jeong,[b] Sung Heum Park*[b] and Myung Ho Hyun*[a]

Received (in Montpellier, France) 9th August 2016,
Accepted 17th October 2016

DOI: 10.1039/c6nj02478e

www.rsc.org/njc

A new wide band gap polymer, P(BDTT–BTBDPPD), consisting of electron rich 4,8-bis(5-(2-ethylhexyl)thiophen-2-yl)benzo[1,2-*b*:4,5-*b*′]dithiophene (BDTT) and electron deficient bithiophene-incorporated bis(pyrrolo[3,4-*c*]-pyrrole-1,3(2*H*,5*H*)-dione) (BTBDPPD) derivative was prepared to improve the photovoltaic performances of a reported polymer, P(BDTT–TBDPPD), containing BDTT and thiophene-incorporated bis(pyrrolo[3,4-*c*]pyrrole-1,3(2*H*,5*H*)-dione) (TBDPPD) derivative. Polymer P(BDTT–BTBDPPD) exhibited maximum absorption at 478 nm and the calculated optical band gap was 2.10 eV. The highest occupied molecular orbital (HOMO) and lowest unoccupied molecular orbital (LUMO) energy levels of P(BDTT–BTBDPPD) were estimated to be −5.44 eV and −3.34 eV. The hole mobility of P(BDTT–BTBDPPD) was 3.22×10^{-4} cm^2 V^{-1} s^{-1}. The polymer solar cells (PSCs) prepared using P(BDTT–BTBDPPD) : $PC_{70}BM$ (1 : 2 wt%) + 3 vol% DIO blend offered a maximum power conversion efficiency (PCE) of 4.62% with an open-circuit voltage (V_{oc}) of 0.90 V, a short-circuit current (J_{sc}) of 7.99 mA cm^{-2}, and a fill factor (FF) of 64%. This study suggests that the replacement of the thiophene spacer unit located between the pyrrolo[3,4-*c*]pyrrole-1,3(2*H*,5*H*)-dione units of bis(pyrrolo[3,4-*c*]pyrrole-1,3(2*H*,5*H*)-dione) derivative with a bithiophene unit did not considerably alter the energy levels and charge transport properties of the resulting polymer. However, the overall photovoltaic performance was improved due mainly to the enhanced morphology of the photoactive layer.

1. Introduction

Polymer solar cells (PSCs) made using blends of electron donating π-conjugated semiconducting polymers[1–5] and electron accepting fullerene derivative[6] have been widely used for solar to electrical energy conversion due to the ease of device fabrication, light weight and low cost for large area device preparation. Literatures reveal that the commercially available [6,6]-phenyl-C_{71}-butyric acid methyl ester ($PC_{70}BM$) is one of the best electron acceptors for the preparation of high energy converting PSCs.[1–35] On the other hand, a variety of copolymers were reported for PSCs, and it was confirmed that the photovoltaic performances of PSCs are highly dependent on the properties of copolymers such as absorption, energy levels, carrier mobility, orientation, molecular weights, crystallinity and interpenetrating network formation along with $PC_{70}BM$.[7–18] Therefore, the development of structurally new π-conjugated semiconducting polymers is crucial to improve the power conversion efficiency (PCE) of polymer solar cells (PSCs). Currently, the conventional PSCs made using polymer:$PC_{70}BM$ blends offer a maximum PCE over 10%;[7–18] the tandem[19–24] and ternary PSCs[25–29] made using two different polymer:$PC_{70}BM$ blends also exhibit a maximum PCE over 10%. The overall PCEs of tandem and ternary PSCs were expected to exceed 25% using appropriate donor polymers due to their advantages such as an improved light absorption *via* the complementary absorptions from two different polymers.[30] We have been interested in the preparation of wide band gap polymers for PSCs because numerous high energy converting low (E_g ~ 1.3–1.6 eV)[1–5,7–12] and medium (E_g ~ 1.6–1.9 eV)[1–5,13–18] band gap polymers have already been reported for PSCs; however, wide band gap polymers (E_g > 1.9 eV)[31–35] are limited.

[a] *Department of Chemistry, Chemistry Institute for Functional Materials, Pusan National University, Busan 690-735, Republic of Korea. E-mail: mhhyun@pusan.ac.kr; Fax: +82-51-516-7421; Tel: +82-51-510-2245*
[b] *Department of Physics, Pukyong National University, Busan 608-737, Republic of Korea. E-mail: spark@pknu.ac.kr; Fax: +82-51-629-5549; Tel: +82-51-629-5774*
[c] *Department of Physics and EHSRC, University of Ulsan, Ulsan 680-749, Republic of Korea*
[d] *Department of Industrial Chemistry, Pukyong National University, Busan 608-739, Republic of Korea*

The very recently reported bis(pyrrolo[3,4-*c*]pyrrole-1,3(2*H*,5*H*)-dione) (BDPPD)-based wide band gap polymer, P(BDTT–TBDPPD), incorporating 4,8-bis(5-(2-ethylhexyl)thiophen-2-yl)benzo[1,2-*b*:4,5-*b*′]dithiophene (BDTT) and thiophene-incorporated bis-(pyrrolo[3,4-*c*]pyrrole-1,3(2*H*,5*H*)-dione) (TBDPPD) derivative showed an optical band gap of 2.08 eV with an intense absorption band between 300 nm and 600 nm.[36] Polymer P(BDTT–TBDPPD) offered a maximum PCE of 3.63% with an open-circuit voltage (V_{oc}) of 0.87 V, a short-circuit current (J_{sc}) of 8.64 mA cm^{-2}, and a fill factor (FF) of 48%. It is worth noting that imide functionalized polymers[2,34,35,37–40] usually showed high PCE due mainly to the enhanced planarity through the conformational locking *via* the S···O interactions between the thienyl sulfur (S) on adjacent electron rich units and the carbonyl oxygen (O) on the imide groups.[2,37] However, the overall PCE of imide functionalized P(BDTT–TBDPPD) is relatively lower compared to that of reported wide band gap polymers.[31–35] The chemical structure along with the possible S···O interactions of P(BDTT–TBDPPD) are displayed in Fig. 1a. We think that the replacement of the thiophene unit positioned between the pyrrolo[3,4-*c*]pyrrole-1,3(2*H*,5*H*)-dione (DPPD) units of TBDPPD with a bithiophene unit might improve the planarity of the resulting bithiophene-incorporated bis(pyrrolo[3,4-*c*]pyrrole-1,3(2*H*,5*H*)-dione) (BTBDPPD) derivative *via* the enhanced S···O interactions, as shown in Fig. 1b. In this instance, we synthesized the polymer P(BDTT–BTBDPPD) containing BDTT and a newly prepared BTBDPPD derivative. The opto-electrical, charge transport and photovoltaic properties of P(BDTT–BTBDPPD) are studied and briefly compared with those of P(BDTT–TBDPPD) to understand the effects of the replacement of thiophene with bithiophene.

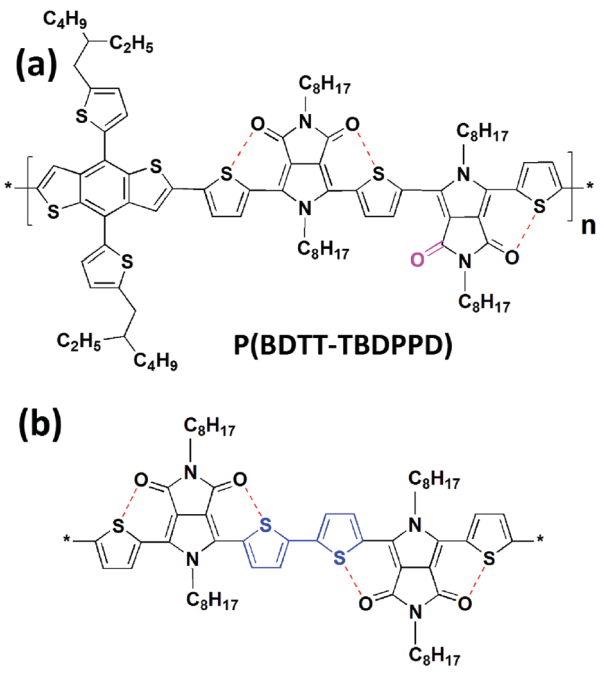

Fig. 1 Chemical structure of P(BDTT–TBDPPD) (a). The possible S···O interactions between the thienyl sulfur (S) and the carbonyl oxygen (O) on bis(pyrrolo[3,4-*c*]pyrrole-1,3-dione) derivatives incorporating thiophene (a) and bithiophene (b) as a connecting spacer unit.

2. Experimental

2.1 Materials and measurements

Reagents were obtained from Sigma-Aldrich. The compounds prepared in this study were purified by column chromatography (silica gel, Merck Kieselgel 60, 70–230 mesh ASTM). The nuclear magnetic resonance (NMR) spectra of the compounds and polymer were recorded on a Varian Mercury Plus spectrometer (300 MHz for ^{1}H and 75 MHz for ^{13}C). The high resolution fast atom bombardment (FAB) mass spectra of the compounds were analyzed using a JEOL JMS-700 mass spectrometer. An Agilent 1200 Infinity Series separation module was used to determine the molecular weights of the polymer using gel permeation chromatography (GPC) with chloroform as an eluent at ambient temperature. The GPC instrument was calibrated with the polystyrene standard prior to analysis. The film state UV-visible absorption spectrum of the polymer was recorded on a JASCO V-570 spectrophotometer, and a CH Instruments Electrochemical Analyzer was used to determine the cyclic voltammogram (CV) of the polymer. The polymer cast film on the platinum working electrode was immersed in an acetonitrile solution containing 0.1 M tetrabutylammonium tetrafluoroborate (Bu_4NBF_4), with Ag/AgCl as a reference electrode and platinum wire as a counter electrode, and the measurement was then performed. Before starting the CV analysis, the instrument was calibrated with the most common ferrocene/ferrocenium ion (Fc/Fc^{+}) standard. Atomic force microscopy (AFM) was performed using a Seiko instruments SPI 3800N-SPA 400.

2.2 Device fabrication and characterization of OFETs

The organic field effect transistors (OFETs) were fabricated on highly n-type-doped silicon (Si) substrates with a 200 nm layer of thermally grown silicon oxide (SiO_2). The Si substrates were subjected to an UV-ozone treatment for 30 min for activation and then treated with an octadecyltrichlorosilane (OTS) self-assembled monolayer. The n-type doped Si substrate functions as a gate electrode and the SiO_2 layer acts as a gate dielectric. The chlorobenzene (CB) solution of the polymer (5 mg mL^{-1}) was spin-cast on top of the Si substrate (2000 rpm) and dried at room temperature (RT) for 30 minutes. The source and drain electrodes (Au, 70 nm) were deposited on top of the polymer layer by thermal evaporation in a vacuum of approximately 2×10^{-6} Torr. The channel length (L) and channel width (W) of the device was 50 μm and 3.0 mm, respectively. The output and transfer characteristics of the OFETs were measured using a Keithley semiconductor parametric analyzer (Keithley 4200). All preparation processes and the characterization of the OFETs were performed inside a N_2-atmosphere glove box. The mobility (μ) was determined using the following equation in the saturation regime:

$$I_{ds,sat} = \mu(WC_i/2L)(V_{gs} - V_T)^2$$

where C_i is the capacitance per unit area of the SiO_2 dielectric (C_i = 15 nF cm^{-2}) and V_T is the threshold voltage.

2.3 Device fabrication and characterization of PSCs

The PSCs were fabricated with the simple device structure of ITO-coated glass substrate/PEDOT:PSS/P(BDTT–BTBDPPD):$PC_{70}BM$/Al. The pre-cleaned ITO-coated glass substrate was dried overnight in an oven. A 40 nm thick layer of PEDOT:PSS (Baytron PH) was spin-cast from an aqueous solution on an ITO-coated glass substrate. The substrate was dried for 10 min at 140 °C in air and then transferred to a glove box to spin-cast the photoactive layer. A solution containing a mixture of P(BDTT–BTBDPPD):$PC_{70}BM$ (1 : 1, 1 : 2 and 1 : 3 wt%) with a total concentration of 20 mg mL^{-1} in chlorobenzene (CB) : 1,8-diiodooctane (DIO) at a volume ratio of 97 : 3 (CB : DIO) was then spin-cast on top of the PEDOT/PSS layer. The film was then dried for 30 min at RT in the glove box. Subsequently, an aluminum (Al, 100 nm) electrode was deposited by thermal evaporation in a vacuum of approximately 3×10^{-6} Torr. The current density–voltage (J–V) characteristics of the PSC devices were measured using a Keithley 2400 Source Measure Unit. The solar cell performance was determined using an Air Mass 1.5 Global (AM 1.5G) solar simulator with an irradiation intensity of 1000 W m^{-2}. The spectral mismatch factor was calculated by comparing the solar simulator spectrum with the AM 1.5 spectrum at RT.

2.4 Synthesis of polymers

Tetraethyl 2,2′-([2,2′-bithiophene]-5,5′-diyl)bis(1-octyl-1*H*-pyrrole-3,4-dicarboxylate) (2). A solution of diethyl 2-bromo-1-octyl-1*H*-pyrrole-3,4-dicarboxylate **1** (1.79 g, 4.45 mmol), which was prepared using the reported procedure,[36] and 5,5′-bis(trimethylstannyl)-2,2′-bithiophene (1.00 g, 2.00 mmol) in toluene (50 mL) was purged with argon for 45 min, and $Pd(PPh_3)_4$ (2 mol%) was then added. The stirred solution was heated to reflux for 15 h under an argon atmosphere. The solution was cooled and the solvent was then removed completely using a rotary evaporator. The residue was dissolved in ethyl acetate (100 mL), washed with a brine solution, and dried over anhydrous Na_2SO_4. The solvent was removed and the compound was purified by column chromatography (silica gel, hexane : ethyl acetate, 70/30, v/v) to afford pure product **2**. Yield: 1.08 g (66%). ^{1}H NMR (300 MHz, $CDCl_3$, δ): 7.33 (s, 2H), 7.14 (s, 2H), 7.00 (s, 2H), 4.23 (q, 8H), 3.86 (t, 4H), 1.55–1.65 (m, 4H), 1.18–1.32 (m, 32H), 0.83 (t, 6H); ^{13}C NMR (75 MHz, $CDCl_3$, δ): 165.1, 163.5, 139.0, 130.9, 129.2, 127.3, 127.2, 123.8, 118.2, 114.9, 60.9, 47.9, 31.7, 31.0, 29.0, 28.9, 26.4, 22.6, 14.1, 14.0; HRMS (ESI) m/z: $[M + H]^+$ calcd for $C_{44}H_{60}N_2O_8S_2$, 808.3791; found, 808.3797.

Tetraethyl 5,5′-([2,2′-bithiophene]-5,5′-diyl)bis(2-bromo-1-octyl-1*H*-pyrrole-3,4-dicarboxylate) (3). NBS (0.48 g, 2.72 mmol) was added in one portion to a stirred solution of compound **2** (1.0 g, 1.24 mmol) in 30 mL of DMF at RT. The solution was stirred for 3 h and then poured in water (150 mL). The solution was extracted twice with diethyl ether (50 mL) and the combined organic layer was washed once with brine and dried over anhydrous Na_2SO_4. The solvent was removed and the compound was purified by column chromatography (silica gel, hexane : ethyl acetate, 80/20, v/v) to afford pure product **3**. Yield: 1.17 g (98%). ^{1}H NMR (300 MHz, $CDCl_3$, δ): 7.18 (s, 2H), 7.05 (s, 2H), 4.10–4.40 (m, 8H), 3.94 (t, 4H), 1.55–1.65 (m, 4H), 1.18–1.38 (m, 32H), 0.85 (t, 6H); ^{13}C NMR (75 MHz, $CDCl_3$, δ): 163.9, 163.2, 139.3, 131.5, 129.0, 127.9, 127.3, 123.9, 115.7, 108.8, 60.9, 46.8, 31.7, 30.5, 29.0, 28.9, 26.4, 22.6, 14.1, 14.0; HRMS (ESI) m/z: $[M + H]^+$ calcd for $C_{44}H_{58}Br_2N_2O_8S_2$, 964.2001; found, 964.2007.

Tetraethyl 5,5′-([2,2′-bithiophene]-5,5′-diyl)bis(1-octyl-2-(thiophen-2-yl)-1*H*-pyrrole-3,4-dicarboxylate) (4). A solution of compound **3** (1.17 g, 1.21 mmol) and 2-(trimethylstannyl)thiophene (0.72 g, 2.40 mmol) in toluene (50 mL) was purged with argon for 45 min, and $Pd(PPh_3)_4$ (2 mol%) was then added. The stirred solution was heated under reflux for 24 h under an argon atmosphere, and the solvent was then removed completely using a rotary evaporator. The residue was dissolved in ethyl acetate (100 mL), washed with a brine solution, and dried over anhydrous Na_2SO_4. The solvent was removed and the compound was purified by column chromatography (silica gel, hexane : ethyl acetate, 70/30, v/v) to afford pure product **4**. Yield: 1.08 g (92%). ^{1}H NMR (300 MHz, $CDCl_3$, δ): 7.49 (d, 2H), 7.04–7.20 (m, 8H), 4.16–4.24 (m, 8H), 3.85 (t, 4H), 1.50–1.60 (m, 4H), 1.06–1.25 (m, 32H), 0.83 (t, 6H); ^{13}C NMR (75 MHz, $CDCl_3$, δ): 164.3, 164.0, 139.2, 131.9, 131.2, 130.4, 129.1, 128.1, 127.7, 127.2, 126.9, 126.0, 123.8, 117.2, 60.7, 45.5, 31.6, 31.0, 29.1, 28.8, 26.3, 22.6, 14.1, 14.0; HRMS (ESI) m/z: $[M + H]^+$ calcd for $C_{52}H_{64}N_2O_8S_4$, 972.3545; found, 972.3551.

Tetraethyl 5,5′-([2,2′-bithiophene]-5,5′-diyl)bis(2-(5-bromothiophen-2-yl)-1-octyl-1*H*-pyrrole-3,4-dicarboxylate) (5). NBS (0.43 g, 2.44 mmol) was added in one portion to a stirred solution of compound **4** (1.08 g, 1.10 mmol) in 25 mL of DMF at RT. The solution was extracted twice with diethyl ether (50 mL) and the combined organic layer was washed once with brine and dried over anhydrous Na_2SO_4. The solvent was removed and the compound was purified by column chromatography (silica gel, hexane : ethyl acetate, 70/30, v/v) to afford pure product **5**. Yield: 1.23 g (98%). ^{1}H NMR (300 MHz, $CDCl_3$, δ): 7.48 (s, 2H), 7.08–7.20 (m, 4H), 6.91 (d, 2H), 4.19 (q, 8H), 3.84 (t, 4H), 1.40–1.50 (m, 4H), 1.08–1.26 (m, 32H), 0.83 (t, 6H); ^{13}C NMR (75 MHz, $CDCl_3$, δ): 164.2, 164.0, 131.2, 131.0, 130.4, 130.0, 129.1, 128.0, 127.8, 127.0, 126.8, 123.8, 117.5, 114.7, 60.8, 45.5, 31.6, 31.1, 29.1, 28.8, 26.3, 22.6, 14.1, 14.0; HRMS (ESI) m/z: $[M + H]^+$ calcd for $C_{52}H_{62}Br_2N_2O_8S_4$, 1128.1756; found, 1128.1762.

5,5′-([2,2′-Bithiophene]-5,5′-diyl)bis(2-(5-bromothiophen-2-yl)-1-octyl-1*H*-pyrrole-3,4-dicarboxylic acid) (6). An aqueous sodium hydroxide (0.87 g in 10 mL water, 22.00 mmol) solution was added to the stirred solution of compound **5** (1.23 g, 1.10 mmol) in methanol : tetrahydrofuran (60 : 30 mL). The solution was heated to 60 °C and stirred for 12 h. Methanol was then removed by rotary evaporation and the residue was dissolved in water (100 mL). The aqueous solution was acidified with 2 N HCl until it became acidic. Then, the mixture was extracted twice with ethyl acetate (50 mL) and the combined organic layer was washed once with water and dried over anhydrous Na_2SO_4. The solvent was removed and the solid material was washed with hexane to afford pure product **6**. Yield: 0.96 g (87%). ^{1}H NMR (300 MHz, acetone-d_6, δ): 7.31 (d, 4H), 7.27 (d, 2H), 7.13 (d, 2H), 3.91 (t, 4H), 1.54–1.66 (m, 4H), 1.05–1.30 (m, 20H), 0.85 (t, 6H); HRMS (ESI) m/z: $[M + H]^+$ calcd for $C_{44}H_{46}Br_2N_2O_8S_4$, 1016.0504; found, 1016.0510.

6,6′-([2,2′-Bithiophene]-5,5′-diyl)bis(4-(5-bromothiophen-2-yl)-5-octyl-1*H*-furo[3,4-*c*]pyrrole-1,3(5*H*)-dione) (7). A solution of compound **6** (0.90 g, 0.88 mmol) in acetic anhydride (60 mL) was stirred at 80 °C overnight. Acetic anhydride was removed completely and the residue was dissolved in ethyl acetate (100 mL). The organic solution was washed once with an aqueous sodium bicarbonate solution (5%) and the organic layer was then dried over anhydrous Na_2SO_4. The solvent was removed and the solid material was washed with hexane to afford pure product **7**. Yield: 0.68 g (78%). ^{1}H NMR (300 MHz, $CDCl_3$, δ): 7.76 (s, 2H), 7.30–7.50 (m, 4H), 7.14 (d, 2H), 4.13 (t, 4H), 1.85–2.00 (m, 4H), 1.06–1.26 (m, 20H), 0.83 (t, 6H); HRMS (ESI) *m*/*z*: $[M + H]^+$ calcd for $C_{44}H_{42}Br_2N_2O_6S_4$, 980.0292; found, 980.0298.

6,6′-([2,2′-Bithiophene]-5,5′-diyl)bis(4-(5-bromothiophen-2-yl)-2,5-dioctylpyrrolo[3,4-*c*]pyrrole-1,3(2*H*,5*H*)-dione) (BTBDPPD). To the ice cold solution of compound **7** (0.45 g, 0.46 mmol) in anhydrous toluene (50 mL) was added 2-octyldodecan-1-amine (0.33 g, 1.10 mmol, in 5 mL toluene) drop-wise through a syringe under an argon atmosphere. The solution was stirred for 1 h at 0 °C and then heated slowly under reflux overnight. Toluene was removed completely and the residue was dissolved in dry methylene chloride (50 mL) and cooled to 0 °C. To the stirred solution, 5 mL of thionyl chloride was added in one portion and heated to 40 °C. After 30 min, the solution was removed completely by rotary evaporation. The pasty mass was dissolved in methylene chloride (50 mL) and washed with brine. The organic layer was dried over anhydrous Na_2SO_4. The solvent was concentrated and the residue was then purified by column chromatography (silica gel, methylene chloride) to afford pure product BTBDPPD. Yield: 0.51 g (72%). ^{1}H NMR (300 MHz, $CDCl_3$, δ): 7.78 (s, 2H), 7.30–7.50 (m, 4H), 7.16 (d, 2H), 4.34 (t, 4H), 3.45 (d, 4H), 1.72–1.88 (m, 6H), 1.06–1.26 (m, 84H), 0.85–0.95 (m, 18H); ^{13}C NMR (75 MHz, $CDCl_3$, δ): 164.2, 164.1, 130.9, 130.8, 130.7, 130.5, 130.1, 128.5, 126.8, 126.1, 124.9, 119.0, 118.7, 114.9, 46.8, 42.5, 37.1, 31.9, 31.7, 31.6, 31.0, 30.0, 29.7, 29.6, 29.4, 29.3, 29.0, 28.8, 26.4, 26.2, 22.7, 22.6, 14.2; HRMS (ESI) *m*/*z*: $[M + H]^+$ calcd for $C_{84}H_{124}Br_2N_4O_4S_4$, 1538.6872; found, 1538.6878.

Polymer P(BDTT–BTBDPPD). A flame-dried, three-neck, round bottom flask containing a solution of monomers BDTT (0.18 g, 0.20 mmol) and BTBDPPD (0.31 g, 0.20 mmol) in CB (20 mL) was purged well with argon for 30 min. Subsequently, Pd_2dba_3 (14 mg) and P(*o*-tol)$_3$ (28 mg) were added and the entire mixture was heated under reflux in argon for 48 h. The solution was cooled to RT and added drop wise to methanol

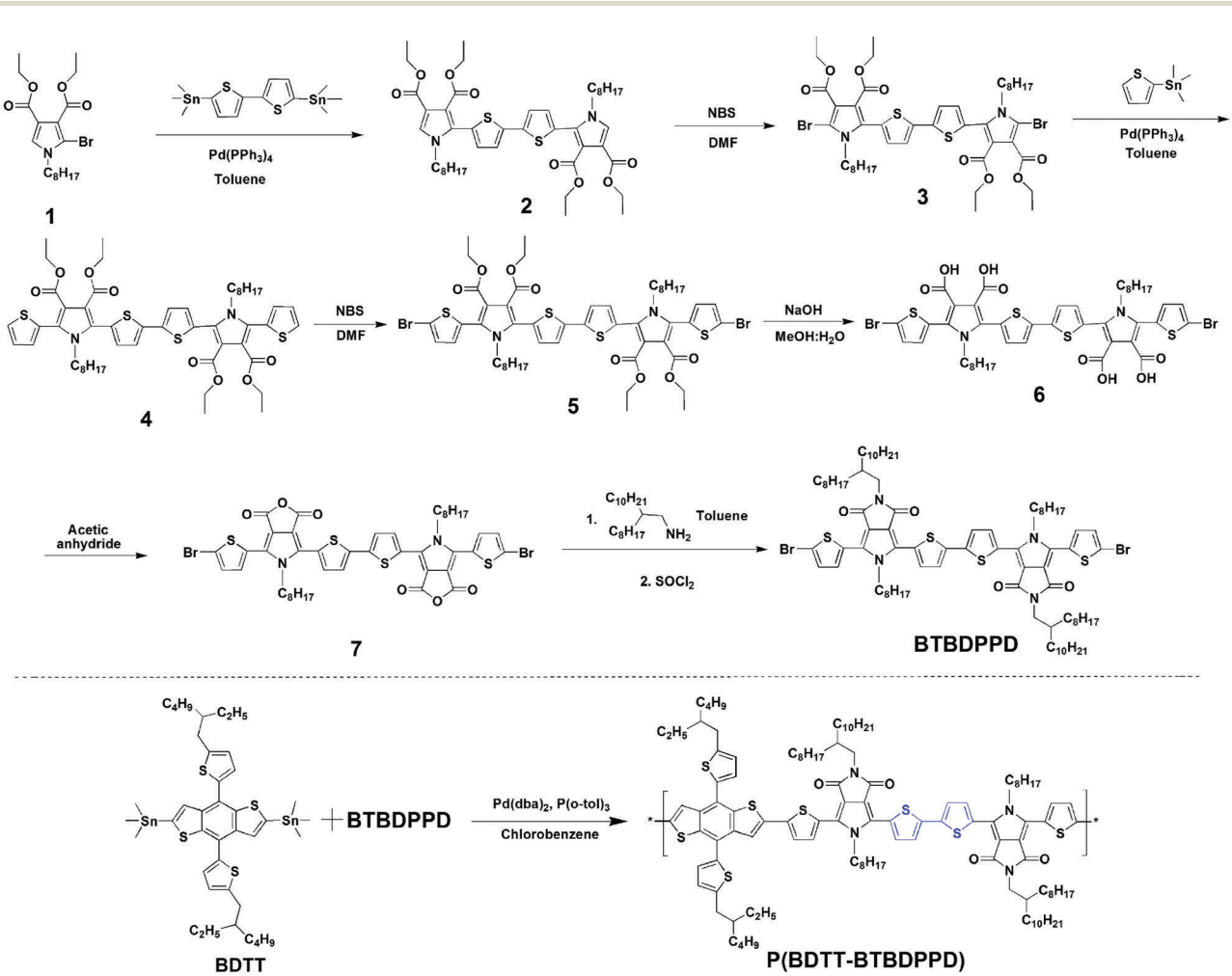

Scheme 1 Synthesis route to monomer BTBDPPD and polymer P(BDTT–BTBDPPD).

Table 1 Molecular weights, opto-electrical and charge transport properties of polymers P(BDT–TBDPPD) and P(BDTT–BTBDPPD)

Polymer name	M_w [b] (g mol^{-1})	PDI[b]	λ_{max} as film[c] (nm)	E_g [d] (eV)	HOMO[e] (eV)	LUMO[f] (eV)	μ[g] (cm^2 V^{-1} s^{-1})
P(BDTT–TBDPPD)[a]	2.57×10^4	1.88	508	2.08	−5.44	−3.36	3.20×10^{-4}
P(BDTT–BTBDPPD)	8.46×10^4	3.24	478	2.10	−5.44	−3.34	3.22×10^{-4}

[a] Data for P(BDT–TBDPPD) are quoted from ref. 36. [b] Weight average molecular weight (M_w) and polydispersity (PDI) of the polymers were determined by GPC using polystyrene standards. [c] Measurements in thin film were performed on the glass substrate. [d] Band gap estimated from the onset wavelength of the optical absorption in thin film. [e] The HOMO level was estimated using cyclic voltammetry analysis. [f] The LUMO level was estimated by the following equation: LUMO = HOMO + E_g. [g] The hole mobility of polymers was estimated from organic field effect transistors.

(250 mL) with constant stirring. The precipitated polymer was then allowed to settle. The precipitates were filtered and washed sequentially with methanol (50 mL) and acetone (50 mL). The polymer was then subjected to Soxhlet extraction with methanol and acetone for 24 h. The remaining solid was dried under vacuum to afford pure polymer P(BDTT–BTBDPPD) as a brown solid. Yield (0.38 g, 97%). ^{1}H NMR (300 MHz, $CDCl_3$, δ): 7.80–7.60 (m, 4H), 7.40–7.20 (m, 6H), 6.90–6.80 (m, 4H), 4.50–4.40 (m, 4H), 3.50–3.40 (m, 4H), 2.90–2.70 (m, 4H), 1.50–1.10 (m, 108H), 1.00–0.70 (m, 30H).

3. Results and discussion

3.1 Synthesis and characterization of polymer

A new electron deficient monomer unit, namely, 6,6′-([2,2′-bithiophene]-5,5′-diyl)bis(4-(5-bromothiophen-2-yl)-2,5-dioctylpyrrolo-[3,4-*c*]pyrrole-1,3(2*H*,5*H*)-dione) (BTBDPPD), and polymer P(BDTT–BTBDPPD) were prepared according to the synthesis route shown in Scheme 1. Polymer P(BDTT–BTBDPPD) showed good solubility in chlorobenzene (CB) and dichlorobenzene (DCB). The estimated weight average (M_w), number average (M_n) molecular weights and polydispersity (PDI) of P(BDTT–BTBDPPD) were 8.46×10^4 g mol^{-1}, 2.60×10^4 g mol^{-1} and 3.24, respectively. The M_w and PDI of P(BDTT–BTBDPPD) are listed in Table 1 along with those of P(BDTT–TBDPPD) for comparison.

3.2 Optical and electrochemical properties

The absorption spectrum of the thin film made from P(BDTT–BTBDPPD) is shown in Fig. 2a. The absorption band covers the region from 300 nm to 600 nm with maximum absorption at 478 nm. The estimated optical band gap (E_g) using the onset absorption wavelength (~590 nm) was 2.10 eV. The improved S···O interaction in P(BDTT–BTBDPPD) was expected to induce a red shift absorption band compared to that of P(BDTT–TBDPPD). However, P(BDTT–BTBDPPD) showed a blue shifted absorption maximum and slightly higher band gap compared to those of P(BDTT–TBDPPD) (λ_{max} ~ 508 nm and E_g ~ 2.08 eV).[36] The combined effects such as lowered electron deficiency and decreased planarity of BTBDPPD due to the presence of a higher number of electron rich thiophene units and the possibility for the unexpected bond twist between the two thiophenes of BTBDPPD, respectively, compared to those of TBDPPD could be the reasons for the blue shift absorption of P(BDTT–BTBDPPD) compared to that of P(BDTT–TBDPPD).

CV analysis was performed to determine the highest occupied and lowest unoccupied molecular orbital (HOMO and LUMO) energy levels of P(BDTT–BTBDPPD). The CV spectrum of P(BDTT–BTBDPPD) is presented in Fig. 2b. The estimated onset oxidation potential ($E_{ox,onset\ vs.\ Ag/AgCl}$) of P(BDTT–BTBDPPD) was 1.12 V from the CV curve. Under the identical condition, the onset oxidation potential of standard ferrocene ($E_{ferrocene\ vs.\ Ag/AgCl}$) was 0.48 V. The HOMO and LUMO levels were calculated to be −5.44 eV and −3.34 eV, respectively, using the standard equations, $E_{HOMO} = [-(E_{ox,onset\ vs.\ Ag/AgCl} - E_{ferrocene\ vs.\ Ag/AgCl}) - 4.8]$ eV and LUMO = HOMO + E_g, respectively. Electrochemical study reveals that the replacement of the thiophene spacer unit located between the DPPD units of TBDPPD with a bithiophene unit did not alter the energy levels much. The absorption maximum and energy levels of P(BDTT–TBDPPD) and P(BDTT–BTBDPPD) are compared in Table 1.

3.3 OFETs characteristics

To determine the semiconducting and charge transport behaviors of P(BDTT–BTBDPPD), organic field effect transistors (OFETs) were

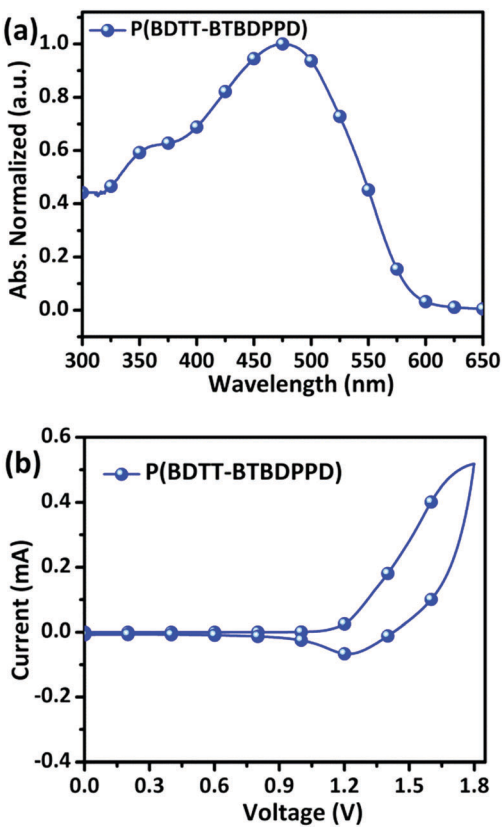

Fig. 2 Absorption spectrum of P(BDTT–BTBDPPD) as thin film (a), and cyclic voltammogram of P(BDTT–BTBDPPD) (b).

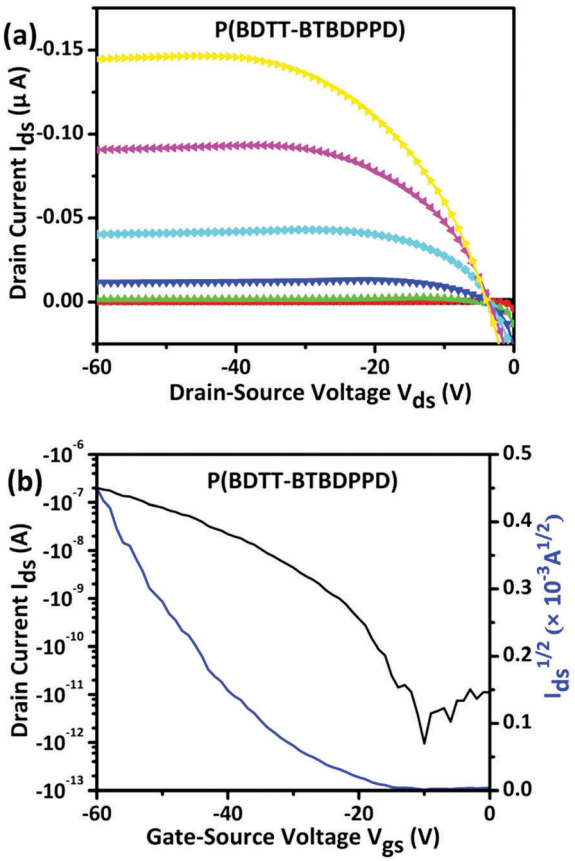

Fig. 3 Typical current–voltage characteristics (drain–source current, I_{ds}, *versus* drain–source voltage, V_{ds}, plots at different voltage (a), and I_{ds} and $I_{ds}^{1/2}$ *versus* gate–source voltage, V_{gs}, plots (b)) for P(BDTT–BTBDPPD)-based OFETs.

fabricated using P(BDTT–BTBDPPD). The typical currentvoltage characteristics (drain–source current, I_{ds}, and drain–source current, $I_{ds}^{1/2}$, *versus* gate–source voltage, V_{gs}, plots) for P(BDTT–BTBDPPD)-based OFETs are presented in Fig. 3. The OFETs characteristics reveal that P(BDTT–BTBDPPD) is a p-type semiconductor and exhibits a maximum field-effect mobility (μ) of 3.22 × 10^{-4} cm^2 V^{-1} s^{-1}. The hole mobility of P(BDTT–BTBDPPD) is found to be similar to that of P(BDTT–TBDPPD) ($\mu \sim 3.20 \times 10^{-4}$ cm^2 V^{-1} s^{-1}).[36] The replacement of the thiophene spacer unit located between the DPPD units of TBDPPD with a bithiophene unit did not change the hole mobility of the resulting polymer much. The hole mobilities of P(BDTT–TBDPPD) and P(BDTT–BTBDPPD) are included in Table 1.

3.4 Polymer solar cell properties

The PSCs were prepared with P(BDTT–BTBDPPD) as an electron donor and $PC_{70}BM$ as an electron acceptor. The PSC device structure and its energy level diagram are shown in Fig. 4a and b, respectively. The *J–V* curves of the PSCs made from P(BDTT–BTBDPPD) : $PC_{70}BM$ (at different ratios) + 3 vol% DIO blends are displayed in Fig. 4c, and their corresponding photovoltaic parameters such as V_{oc}, J_{sc}, FF and PCE are summarized in Table 2. The addition of processive additives such as DIO has been reported to significantly boost the PSC device efficiency *via* controlling the morphology of the photoactive layer.[41] For example, previously reported imide functionalized polymers (DPPD and TPD-based polymers) showed poor performance when the PSC device was made without DIO, however the performance was greatly improved *via* controlling the morphology of the photoactive layer using 3 vol% DIO as a processive additive.[34–36,42,43] Consequently, we prepared PSCs using 3 vol% DIO as an additive to control the morphology of the photoactive layer. The PSCs made from the 1 : 2 wt% blend offered a maximum PCE of 4.62% with a V_{oc} of 0.90 V, a J_{sc} of 7.99 mA cm^{-2}, and a FF of 64%. The V_{oc} and FF achieved for P(BDTT–BTBDPPD) are found to be reasonably high compared to those of efficient polymers reported for PSCs.[7–36] However, the wide band gap of P(BDTT–BTBDPPD) limits the photocurrent of PSCs and restricts the PCE to less than 5%. The incident photon to the collected electron (IPCE) spectra of the PSC made using P(BDTT–BTBDPPD) : $PC_{70}BM$ (1 : 2 wt%) + 3 vol% DIO blend was measured to validate the J_{sc} value achieved for P(BDTT–BTBDPPD)-based PSC.

The IPCE spectrum is shown in Fig. 4d. The IPCE responses cover the region from 300 nm to 700 nm with maximum IPCE of 66% at 460 nm, and the integrated J_{sc} value of the IPCE curve and the J_{sc} value obtained from the *J–V* curve are comparable with each other.

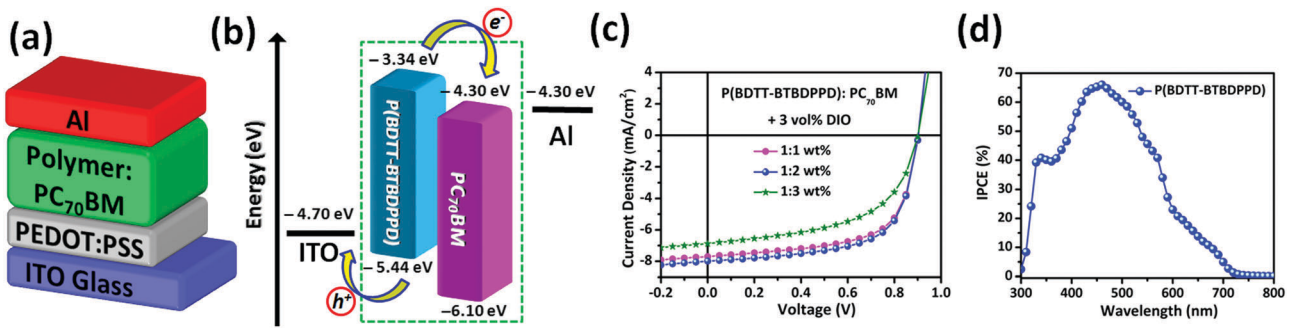

Fig. 4 The PSC device structure (a), the energy level diagram for the materials used for PSC fabrication (b), the *J–V* characteristics of the PSCs prepared using P(BDTT–BTBDPPD) : $PC_{70}BM$ (at different ratio) + 3 vol% DIO blends (c), and the IPCE spectrum of the PSC made using P(BDTT–BTBDPPD) : $PC_{70}BM$ (1 : 2 wt%) + 3 vol% DIO blend (d).

Table 2 Photovoltaic properties of the PSCs prepared using the configuration of ITO/PEDOT:PSS/P(BDTT–BTBDPPD) : $PC_{70}BM$ (at different ratios) + 3 vol% DIO/Al

Ratio (wt%)	V_{oc} [a] (V)	J_{sc} [b] (mA cm^{-2})	FF[c] (%)	PCE[d] (%)
1 : 1	0.90	7.70	64	4.45
1 : 2	0.90	7.99	64	4.62
1 : 3	0.90	6.88	54	3.34

[a] Open-circuit voltage. [b] Short-circuit current density. [c] Fill factor. [d] Power conversion efficiency.

The comparison of the photovoltaic performance of P(BDTT–BTBDPPD) with that of P(BDTT–TBDPPD) reveals that the connecting spacer unit positioned between the pyrrolo[3,4-*c*]pyrrole-1,3(2*H*,5*H*)-dione units of bis(pyrrolo[3,4-*c*]pyrrole-1,3(2*H*,5*H*)-dione) affects the photovoltaic performance notably. The maximum photovoltaic performance reported for P(BDTT–TBDPPD) was 3.63% with a V_{oc} of 0.87 V, a J_{sc} of 8.64 mA cm^{-2}, and a FF of 48%.[36] The V_{oc} obtained for the PSCs made from P(BDTT–TBDPPD) and P(BDTT–BTBDPPD) are quite similar since the HOMO energy levels of both polymers P(BDTT–TBDPPD) and P(BDTT–BTBDPPD) are identical. On the other hand, the J_{sc} of P(BDTT–BTBDPPD)-based PSC is somewhat lower than that of P(BDTT–TBDPPD)-based PSC, and the lower J_{sc} is expected due to the blue shift absorption of P(BDTT–BTBDPPD) compared to that of P(BDTT–TBDPPD). Interestingly, the maximum FF achieved for P(BDTT–BTBDPPD)-based PSC is significantly higher than that of P(BDTT–TBDPPD)-based PSC. The FF is usually correlated with the hole mobility of the donor polymer and mainly with the surface morphology of the photoactive layer. The hole mobilities of both polymers P(BDTT–TBDPPD) and P(BDTT–BTBDPPD) are found to be similar, and consequently, the higher FF is expected to originate from the different morphologies of the photoactive layers. In this instance, we investigated the atomic force microscopy (AFM) images of the film made from P(BDTT–BTBDPPD) : $PC_{70}BM$ (1 : 2 wt%) + 3 vol% DIO blend, and the corresponding topology and phase AFM images are presented in Fig. 5. The AFM images reveal that the phase separation between P(BDTT–BTBDPPD) and $PC_{70}BM$ was excellent, which is beneficial for efficient carrier transport and separation. The comparison of the AFM images of films made from P(BDTT–TBDPPD):$PC_{70}BM$[36] and P(BDTT–BTBDPPD) : $PC_{70}BM$ blends reveals that the morphology was completely changed when the connecting spacer unit was changed from thiophene to bithiophene. As stated above, the improved phase separation of P(BDTT–BTBDPPD) and $PC_{70}BM$ allows better charge transport and collection, and consequently offers high FF. We believe that P(BDTT–BTBDPPD) could be an efficient wide band gap polymer for PSCs utilizing high energy areas of sunlight. In addition, the incorporation of strong electron acceptor units such as 2,1,3-benzothiadiazole (BT), thieno[3,4-*c*]pyrrole-4,6-dione (TPD), thieno[3,4-*b*]thiophene (TT) and pyrrolo[3,4-*c*]pyrrole-1,4-dione (DPP) derivatives instead of a bithiophene connecting spacer unit is expected to give high energy converting low band gap tercopolymers for PSCs.

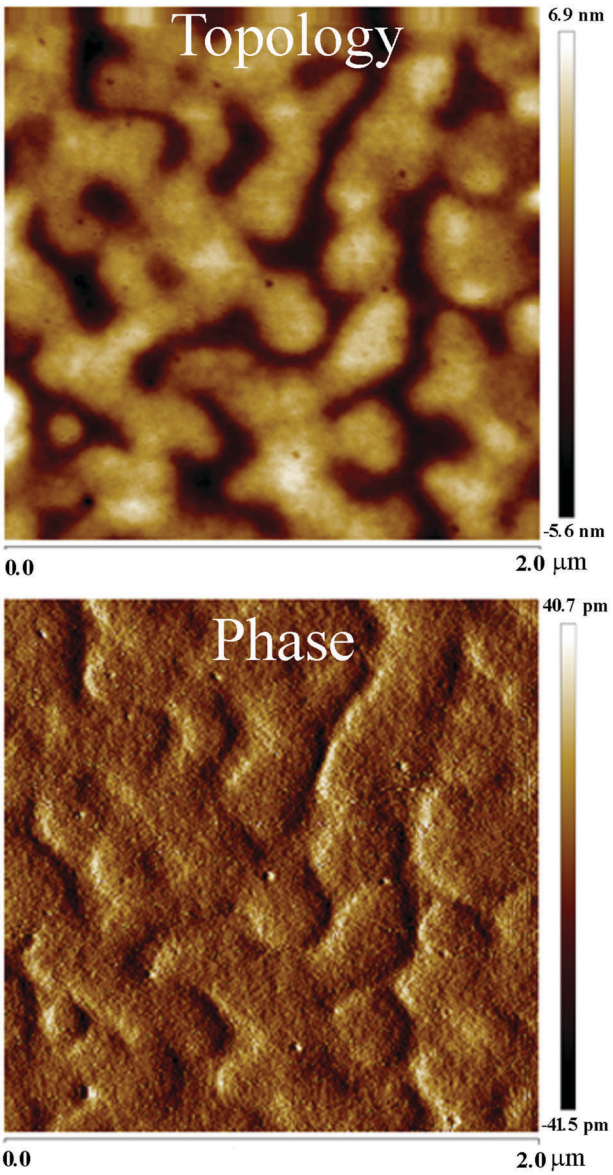

Fig. 5 Topology and phase AFM images of the film made from P(BDTT–BTBDPPD) : $PC_{70}BM$ (1 : 2 wt%) + 3 vol% DIO blend.

4. Conclusions

Polymer P(BDTT–BTBDPPD) was prepared to investigate the effect of changing the connecting spacer unit located between the pyrrolo[3,4-*c*]pyrrole-1,3(2*H*,5*H*)-dione units of bis(pyrrolo[3,4-*c*]-pyrrole-1,3(2*H*,5*H*)-dione)-based polymers. The copolymerization of electron rich BDTT and newly prepared electron deficient BTBDPPD afforded polymer P(BDTT–BTBDPPD). The estimated E_g, HOMO and LUMO levels of P(BDTT–BTBDPPD) were 2.10 eV, −5.44 eV and −3.34 eV, respectively. The OFETs and PSCs made using P(BDTT–BTBDPPD) exhibited a mobility of 3.22 × 10^{-4} cm^2 V^{-1} s^{-1} and a PCE of 4.62% (V_{oc} ∼ 0.90 V, J_{sc} ∼ 7.99 mA cm^{-2}, and FF ∼ 64%). This study suggests that the replacement of a thiophene spacer unit with a bithiophene unit induced a blue shifted absorption maximum, but the band gap, energy levels and hole mobility remained same for the resulting

polymer. Interestingly, the overall photovoltaic performance of bithiophene-incorporated bis(pyrrolo[3,4-*c*]pyrrole-1,3(2*H*,5*H*)-dione)-based polymer is notably improved compared to that of thiophene-incorporated bis(pyrrolo[3,4-*c*]pyrrole-1,3(2*H*,5*H*)-dione)-based polymer. The morphology changes were recognized as a main reason for the enhanced PCE. We believe that this study will be helpful to develop efficient polymers *via* the incorporation of more suitable connecting spacer units on the backbone of bis(pyrrolo[3,4-*c*]pyrrole-1,3(2*H*,5*H*)-dione) unit.

Acknowledgements

This research was supported by the National Research Foundation of Korea (NRF-2013R1A2A2A04014576). S. C. acknowledges the support by the National Research Foundation of Korea (NRF-2014R1A4A1071686).

Notes and references

1 L. Lu, T. Zheng, Q. Wu, A. M. Schneider, D. Zhao and L. Yu, *Chem. Rev.*, 2015, **115**, 12666.
2 X. Guo, A. Facchetti and T. J. Marks, *Chem. Rev.*, 2014, **114**, 8943.
3 C. Gao, L. Wang, X. Li and H. Wang, *Polym. Chem.*, 2014, **5**, 5200.
4 P. Deng and Q. Zhang, *Polym. Chem.*, 2014, **5**, 3298.
5 A. Pron and M. Leclerc, *Prog. Polym. Sci.*, 2013, **38**, 1815.
6 L. Huo and J. Hou, *Polym. Chem.*, 2011, **2**, 2453.
7 J. You, L. Dou, K. Yoshimura, T. Kato, K. Ohya, T. Moriarty, K. Emery, C.-C. Chen, J. Gao, G. Li and Y. Yang, *Nat. Commun.*, 2013, **4**, 1446.
8 Z. He, B. Xiao, F. Liu, H. Wu, Y. Yang, S. Xiao, C. Wang, T. P. Russell and Y. Cao, *Nat. Photonics*, 2015, **9**, 174.
9 J.-D. Chen, C. Cui, Y.-Q. Li, L. Zhou, Q.-D. Ou, C. Li, Y. Li and J.-X. Tang, *Adv. Mater.*, 2015, **27**, 1035.
10 L. Dou, J. Gao, E. Richard, J. You, C.-C. Chen, K. C. Cha, Y. He, G. Li and Y. Yang, *J. Am. Chem. Soc.*, 2012, **134**, 10071.
11 L. Dou, W.-H. Chang, J. Gao, C.-C. Chen, J. You and Y. Yang, *Adv. Mater.*, 2013, **25**, 825.
12 E. Wang, W. Mammo and M. R. Andersson, *Adv. Mater.*, 2014, **26**, 1801.
13 J. Zhao, Y. Li, G. Yang, K. Jiang, H. Lin, H. Ade, W. Ma and H. Yan, *Nat. Energy*, 2016, **1**, 15027.
14 C. Duan, A. Furlan, J. J. v. Franeker, R. E. M. Willems, M. M. Wienk and R. A. J. Janssen, *Adv. Mater.*, 2015, **27**, 4461.
15 Y. Liu, J. Zhao, Z. Li, C. Mu, W. Ma, H. Hu, K. Jiang, H. Lin, H. Ade and H. Yan, *Nat. Commun.*, 2014, **5**, 5293.
16 K. Li, Z. Li, K. Feng, X. Xu, L. Wang and Q. Peng, *J. Am. Chem. Soc.*, 2013, **135**, 13549.
17 J.-H. Kim, J. B. Park, I. H. Jung, A. C. Grimsdale, S. C. Yoon, H. Yang and D.-H. Hwang, *Energy Environ. Sci.*, 2015, **8**, 2352.
18 N. Wang, Z. Chen, W. Wei and Z. Jiang, *J. Am. Chem. Soc.*, 2013, **135**, 17060.
19 C.-C. Chen, W.-H. Chang, K. Yoshimura, K. Ohya, J. You, J. Gao, Z. Hong and Y. Yang, *Adv. Mater.*, 2014, **26**, 5670.
20 J.-H. Kim, J. B. Park, F. Xu, D. Kim, J. Kwak, A. C. Grimsdale and D.-H. Hwang, *Energy Environ. Sci.*, 2014, **7**, 4118.
21 J. Youa, L. Doua, Z. Hongc, G. Li and Y. Yang, *Prog. Polym. Sci.*, 2013, **38**, 1909.
22 W. Li, A. Furlan, K. H. Hendriks, M. M. Wienk and R. A. J. Janssen, *J. Am. Chem. Soc.*, 2013, **135**, 5529.
23 L. Dou, J. You, J. Yang, C.-C. Chen, Y. He, S. Murase, T. Moriarty, K. Emery, G. Li and Y. Yang, *Nat. Photonics*, 2012, **6**, 180.
24 J. You, L. Dou, K. Yoshimura, T. Kato, K. Ohya, T. Moriarty, K. Emery, C.-C. Chen, J. Gao, G. Li and Y. Yang, *Nat. Commun.*, 2013, **4**, 1446.
25 L. Lu, M. A. Kelly, W. You and L. Yu, *Nat. Photonics*, 2015, **9**, 491.
26 L. Lu, T. Xu, W. Chen, E. S. Landry and L. Yu, *Nat. Photonics*, 2014, **8**, 716.
27 T. Ameri, P. Khoram, J. Min and C. J. Brabec, *Adv. Mater.*, 2013, **25**, 4245.
28 P. Cheng, Y. Li and X. Zhan, *Energy Environ. Sci.*, 2014, **7**, 2005.
29 L. Lu, T. Xu, W. Chen, E. S. Landry and L. Yu, *Nat. Photonics*, 2014, **8**, 716.
30 R. R. Lunt, T. P. Osedach, P. R. Brown, J. A. Rowehl and V. Bulovic, *Adv. Mater.*, 2011, **23**, 5712.
31 X. Guo, C. Cui, M. Zhang, L. Huo, Y. Huang, J. Hou and Y. Li, *Energy Environ. Sci.*, 2012, **5**, 7943.
32 S. H. Park, A. Roy, S. Beaupré, S. Cho, N. Coates, J. S. Moon, D. Moses, M. Leclerc, K. Lee and A. J. Heeger, *Nat. Photonics*, 2009, **3**, 297.
33 W. Li, L. Yang, J. R. Tumbleston, L. Yan, H. Ade and W. You, *Adv. Mater.*, 2014, **26**, 4456.
34 V. Tamilavan, K. H. Roh, R. Agneeswari, D. Y. Lee, S. Cho, Y. Jin, S. H. Park and M. H. Hyun, *J. Polym. Sci., Part A: Polym. Chem.*, 2014, **52**, 3564.
35 V. Tamilavan, K. H. Roh, R. Agneeswari, D. Y. Lee, S. Cho, Y. Jin, S. H. Park and M. H. Hyun, *J. Mater. Chem. A*, 2014, **2**, 20126.
36 R. Agneeswari, I. Shin, V. Tamilavan, D. Y. Lee, S. Cho, Y. Jin, S. H. Park and M. H. Hyun, *Org. Electron.*, 2016, **30**, 253.
37 X. Guo, N. Zhou, S. J. Lou, J. W. Hennek, R. P. Ortiz, M. R. Butler, P.-L. T. Boudreault, J. Strzalka, P.-O. Morin, M. Leclerc, J. T. L. Navarrete, M. A. Ratner, L. X. Chen, R. P. H. Chang, A. Facchetti and T. J. Marks, *J. Am. Chem. Soc.*, 2012, **134**, 18427.
38 N. Zhou, X. Guo, R. P. Ortiz, S. Li, S. Zhang, R. P. H. Chang, A. Facchetti and T. J. Marks, *Adv. Mater.*, 2012, **24**, 2242.
39 C. Cabanetos, A. E. Labban, J. A. Bartelt, J. D. Douglas, W. R. Mateker, J. M. J. Frechet, M. D. McGehee and P. M. Beaujuge, *J. Am. Chem. Soc.*, 2013, **135**, 4656.
40 C. E. Small, S. Chen, J. Subbiah, C. M. Amb, S.-W. Tsang, T.-H. Lai, J. R. Reynolds and F. So, *Nat. Photonics*, 2012, **6**, 115.
41 H.-C. Liao, C.-C. Ho, C.-Y. Chang, M.-H. Jao, S. B. Darling and W.-F. Su, *Mater. Today*, 2013, **16**, 326.
42 T.-Y. Chu, J. Lu, S. Beaupre, Y. Zhang, J.-R. Pouliot, S. Wakim, J. Zhou, M. Leclerc, Z. Li, J. Ding and Y. Tao, *J. Am. Chem. Soc.*, 2011, **133**, 4250.
43 C. M. Amb, S. Chen, K. R. Graham, J. Subbiah, C. E. Small, F. So and J. R. Reynolds, *J. Am. Chem. Soc.*, 2011, **133**, 10062.

